Long-Term Fermi Observations of Markarian 421: Physical Clues

Bidzina Kapanadze

- E. Kharadze National Astrophysical Observatory (Abastumani, Georgia)
- Space Research Center, Ilia State University (Tbilisi, Georgia)
- INAF, Osservatorio Astronomico di Brera (Merate, Italy)

2024 September 10, University of Maryland

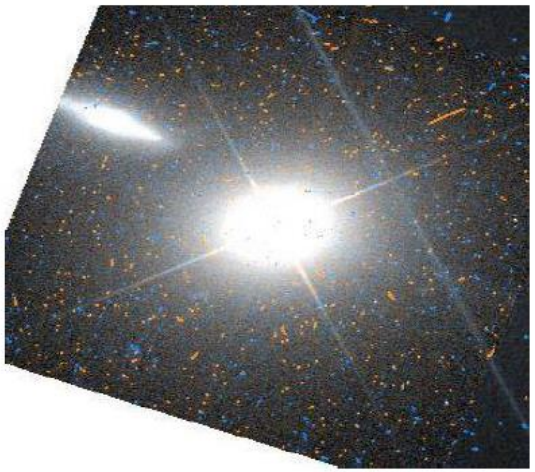

HST optical image (Scarpa+2000)

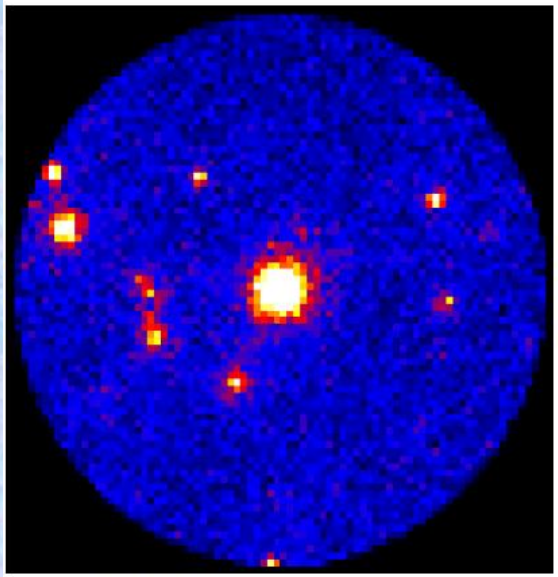

0.3-300 GeV image

Mrk 421

- Active nucleus of bright elliptical galaxy with effective radius of 6.64 kpc (Wu+2000)
- HBL source situated at z=0.031
- The first extragalactic TeV-detected source (Punch +1992), and regularly observed in this energy range afterwards (Gaidos+1996, Aharonian+1999, 2002, 2003,2005,2007; Acciari+2009,2011,2014; Aielli+2010; Aleksic+2010,2012, 2015a,2015b; Bartoli+2011,2016; Balokovic+2016 etc.)
- Highest-energy photon with E >10 TeV (Okomura+2002)
- Extreme VHE flux variability (e.g. Gaiodos+1996)
- The brightest HBL in the 0.3—10 keV and 0.3--300 GeV bands
- **My "favorite" target** (2020ApJS..247...27K, 2019hepr.confE..15K, 2018ApJ...858...68K, 2018ApJ...854...66K, 2017ApJ...848..103K, 2017AIPC.1792e0021K, 2016ApJ...831..102K, 2016frap.confE..33K, 2014ies..conf..116K Atels#16062,9137, 7654, 4918, 4864, 4792)

- 0.3—300 GeV photon flux frequently higher than 10^7 ph/cm^2/s: observed very rarely for other HBLs.
- The highest 0.3—300 GeV photon flux $\approx 10^6$ ph/cm^2/s (2013 April 15, during two subsequent 1-hr detections during (56397.)33–42)
- Detectable even on intraday timescales during the strongest high-energy flares down to 0.6 hr (on 2012 July 16; MJD (56124.)47–50)

- Detections with TS≥9 & Npr≥8 for different time bins
  - ✓ 1-week: 99.5% 4-d: 95% 3-d: 90% 2-d: 86% 1-d: 51%

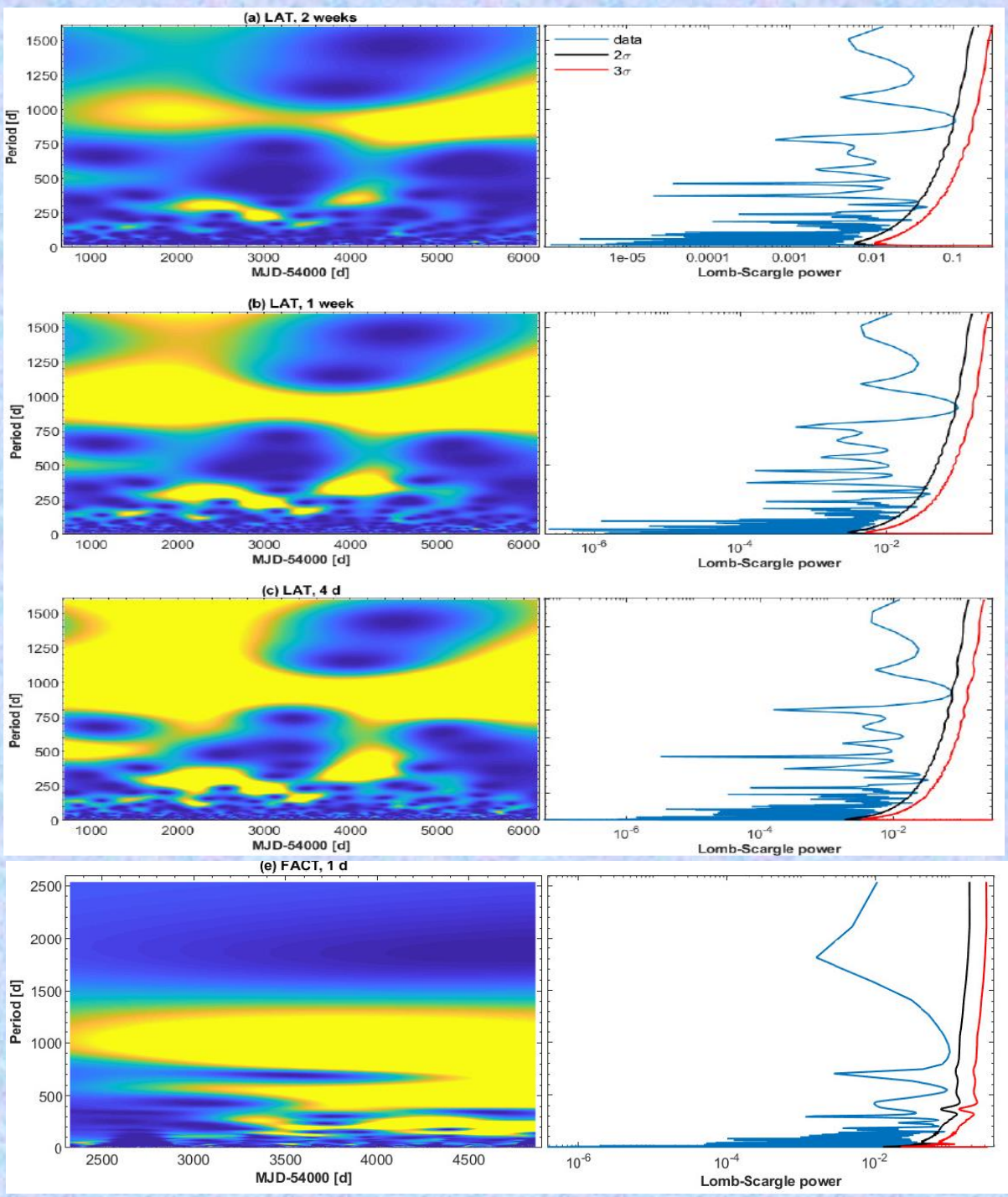

- Non-periodic HE and VHE variability at ≥ 3σ significance (contrary to some earlier claims: Bhata & Dhital 2020; Gupta+2019; Sandrineli+2017) ➔
- No hints at the central SMBH presence or at the jet helicity ➔
- Erratic propagation of relativistic shocks of different strengths through the jet pointed to the observer (Kapanadze+2016, 2017, 2018a, 2018b, 2020, 2024)

- **Various levels of the 0.3—300 GeV flaring activity in different periods**

				0.3–300 GeV				0.3–1 GeV	1–10 GeV	10–100 GeV
Per.	Dates (UTC)	MJDs	Activ. level	F_{max}	F_{min}	F_{mean}	F_{var}	F_{mean}	F_{mean}	F_{mean}
(1)	(2)	(3)	(4)	(5)	(6)	(7)	(8)	(9)	(10)	(11)
1	2008-09-10–2009—03-14	(54)720–910	Low-3	8.01(1.88)	3.66(0.72)	6.30(0.16)	11.3(3.4)	3.91(0.10)	2.01(0.06)	0.36(0.03)
2	2009-03-15–2010-07-31	54911–55409	Medium-2	13.80(1.72)	3.76(0.77)	7.72(0.11)	25.3(1.6)	4.55(0.08)	2.62(0.05)	0.44(0.03)
3	2010-08-01–2011-06-17	(55)410–730	Medium-3	12.47(1.34)	2.43(0.57)	7.39(0.14)	29.0(2.2)	4.48(0.08)	2.39(0.05)	0.42(0.03)
4	2011-06-18–2012-02-29	(55)731–987	Low-2	11.34(1.35)	2.43(0.57)	6.72(0.14)	24.6(2.4)	4.05(0.07)	2.30(0.05)	0.37(0.03)
5	2012-03-01–10-15	55988–56216	Highest-1	32.47(2.33)	4.62(0.70)	14.04(0.23)	60.4(1.8)	8.45(0.15)	4.65(0.09)	0.83(0.05)
6	2012-10-17–2013-10-25	(56)216–589	Highest-2	27.54(2.24)	3.93(0.88)	12.89(0.18)	51.7(1.5)	7.76(0.10)	4.30(0.06)	0.67(0.04)
7	2013-10-26–2014-08-19	(56)590–888	High-1	20.03(1.83)	2.25(0.80)	9.40(0.19)	36.3(2.1)	6.19(0.11)	3.08(0.06)	0.49(0.04)
8	2014-08—20–2016-09-18	56889–57649	High-2	16.79(1.70)	1.91(0.69)	8.46(0.10)	34.8(1.6)	4.88(0.06)	2.89(0.04)	0.54(0.03)
9	2016-09-20–2017-07-02	(57)650–937	High-4	15.35(1.39)	2.14(0.63)	6.57(0.15)	38.2(2.6)	4.14(0.08)	1.99(0.05)	0.32(0.03)
10	2017-07-03–2018-07-25	57938–58325	Highest-3	22.41(1.86)	2.20(0.63)	7.85(0.16)	47.9(2.2)	4.89(0.08)	2.47(0.05)	0.40(0.03)
11	2018-08-01–2021-01-31	58331–59245	Medium-1	15.00(2.72)	3.00(0.68)	7.17(0.09)	29.7(1.4)	4.46(0.06)	2.29(0.04)	0.37(0.02)
12	2021-02-01–2022-05-31	(59)246–695	Low-1	11.96(2.07)	2.29(0.53)	6.72(0.12)	24.8(2.3)	4.28(0.07)	2.08(0.04)	0.31(0.02)
13	2022-06-01–2023-08-01	59696–60157	High-3	16.01(1.58)	2.80(0.72)	9.50(0.14)	33.6(1.7)	6.09(0.10)	2.90(0.06)	0.55(0.04)

	LAT, >100 GeV			
Per.	N_{pred}	TS	F_{mean}	Γ
(1)	(2)	(3)	(4)	(5)
1	17	267	5.36(0.65)	2.11(0.14)
2	29	443	5.27(0.53)	1.79(0.09)
3	8	115	2.09(0.18)	2.27(0.24)
4	3	50	1.04(0.24)	2.20(0.28)
5	10	119	4.28(0.72)	1.95(0.16)
6	28	413	7.17(0.74)	2.31(0.13)
7	18	255	5.29(0.66)	1.78(0.15)
8	37	480	4.19(0.40)	1.76(0.09)
9	8	105	1.46(0.43)	1.62(0.17)
10	16	229	4.45(0.57)	1.68(0.11)
11	51	728	5.39(0.47)	1.94(0.07)
12	17	248	3.19(0.39)	1.70(0.10)
13	25	345	5.78(0.65)	1.67(0.09)

- LAT-band fluxes: 10^{-8} ph/cm^2/s
- F_{max}, F_{min}, F_{mean}: maximum, minimum & mean photon fluxes
- Fvar: farctional variability amplitude (%)
- Γ: power-law photon index

- **0.3–300 GeV range** (Abdo+2010, 2011)
  - **Larger LAT effective area (>0.5 m²)**
  - **Relatively good angular resolution (the 68% containment angle <2 vs 3.5 at 00 MeV);**
  - **Minimized contamination from misclassified cosmic rays ➔ Smaller systematic errors & spectral fit less sensitive to the contamination from unaccounted, transient neighbouring sources ➔ Highest S/N e ratio for the Mrk 21 with the higher-energy SED peak mostly beyond 300 GeV**

- 2012 June–September: strongest LAT-band flaring activity - enhanced matter collimation rate through the jet pointed to the observer?
-

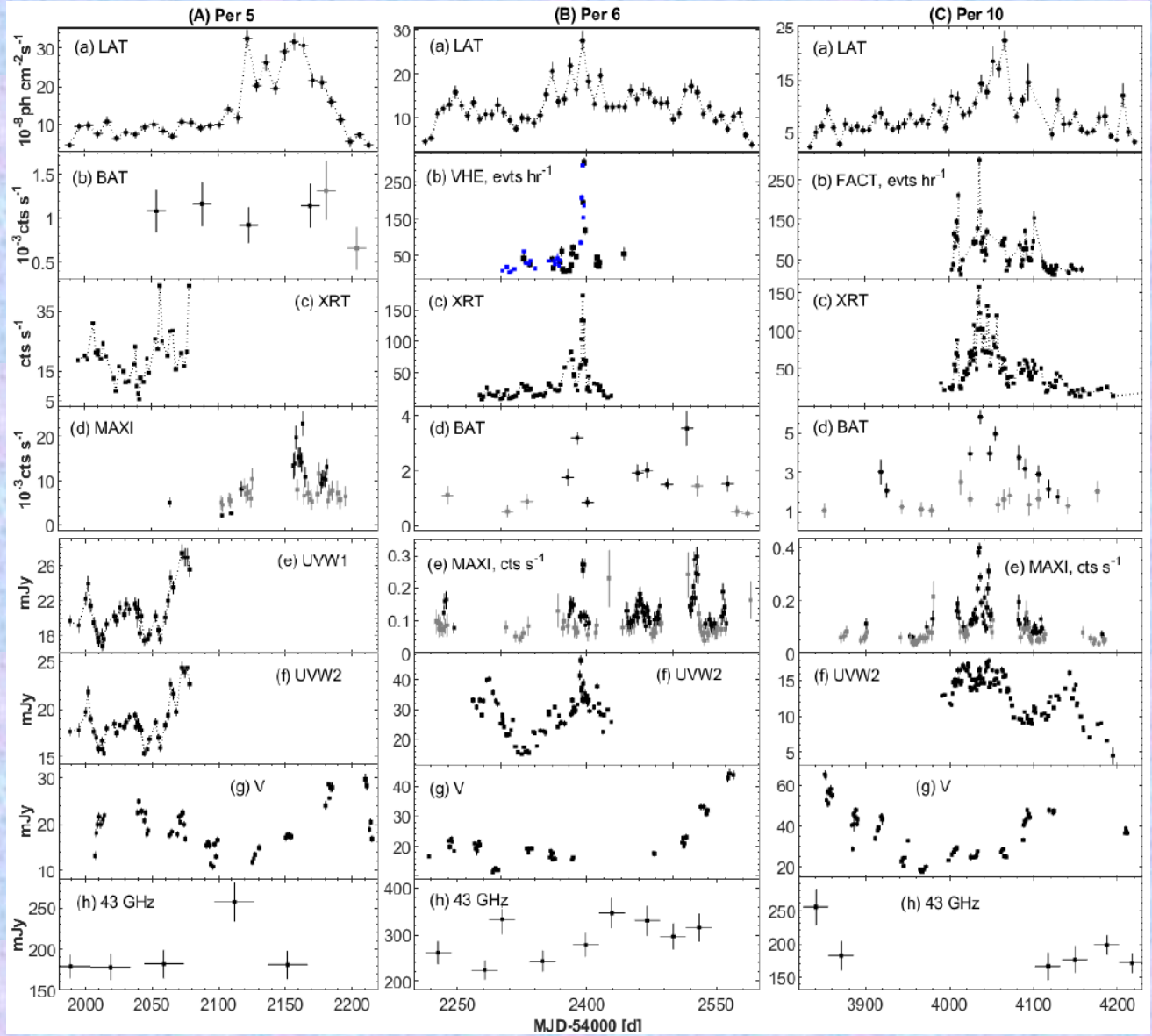

- Highest historical 0.3–300 GeV flux (integrations times of 1-d and longer)
- No Swift XRT and UVOT observations (seasonal Sun restriction for Swift)
- Moderate MAXI-band flaring activity
- Only two 5σ-detections with BAT
- No observations with any Cherenkov-type telescope
- Relatively elevated radio-to-optical states
- Relatively moderate 100-500 GeV activity detected with LAT ➔ Most of the flaring activity at the energies E<10 GeV ➔
- Highly enhanced collimation rate for electrons capable to upscatter radio-to-optical photons in the Thomson regime?

- Short-term LAT-band flares during 2012 June–September: one symmetric; positive or negative asymmetries – 3 instances per each; 2 – double-peaked
  - ✓Symmetric shape: observed variability driven by the crossing time-scale of the underlying disturbance (shock front; Roy+2019; Nalewajko 2013)

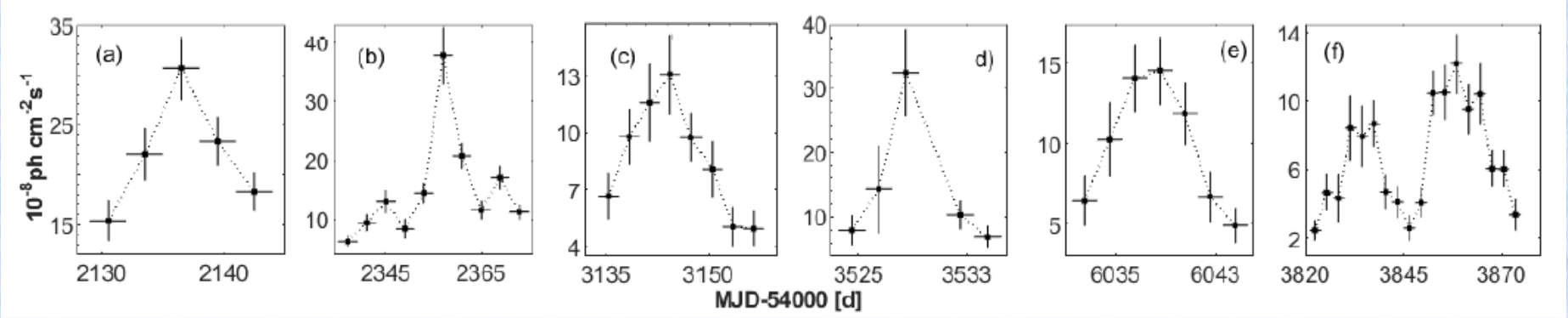

✓ Negative asymmetry: gradual acceleration of the particles responsible for the IC upscattering of low-energy photons to the MeV–GeV range ➔ Cooling time-scale shorter than the acceleration one ➔ Inherent to the stochastic (Fermi II) mechanism operating in the jet region with low magnetic field and high matter density (Virtanen & Vainio 2005)

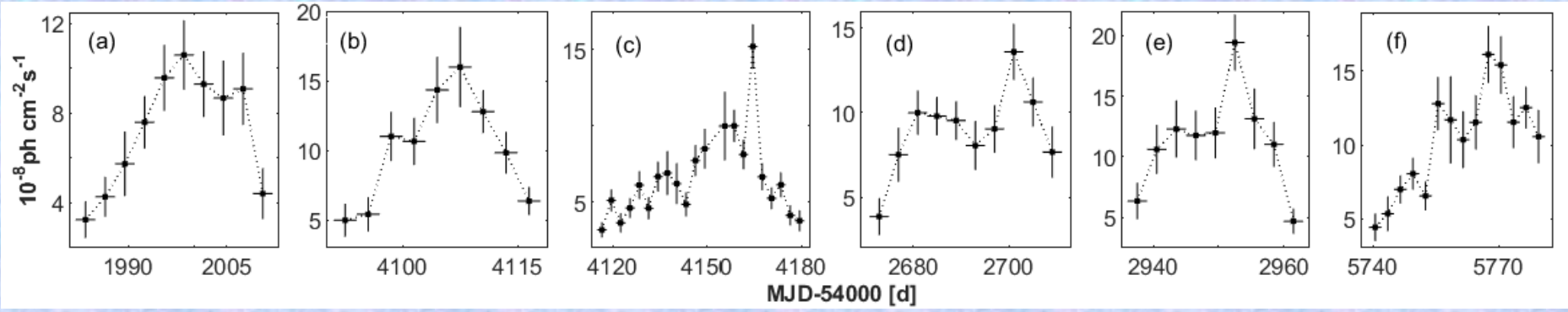

✓ Positive asymmetry: nonuniformity of the Doppler factor across the jet, caused by the radial expansion of the relativistic flow ➔ Significant symmetry distortion of the observed light curves

❖ Caution: smaller variance of the Doppler factor across the emitting shell with decreasing jet opening angle ➔ Decline in the flare asymmetry ➔ Observation of symmetric flare profile for the jet opening angle $\theta \lesssim 0.3$ deg

✓ Alternative origin of positively-asymmetric flares: fast injection of accelerated particles and slower radiative cooling and/or escape from the energization region ➔ Cooling-dominated variability

❖ Caution: very short radiative lifetimes corresponding to the X-ray to MeV–GeV energy range ➔ If the emitting shells are not considerably extended in the jet radial direction during the particular flare, the observed positively-asymmetric profile can by produced by superposition of two or more low-amplitude events

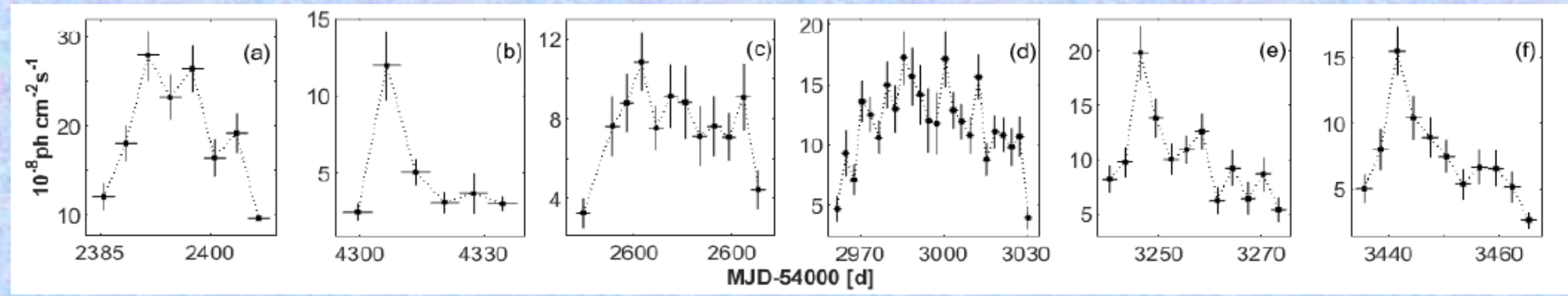

✓ Two-peak flare: propagation of forward and reverse shocks ➔ Triggered by colliding 'shells' of high-energy plasma, injected into the blazar jet with different speeds: a forward shock moving into the slower shell and a reverse one propagating in the faster shell (Bottcher & Dermer 2010)

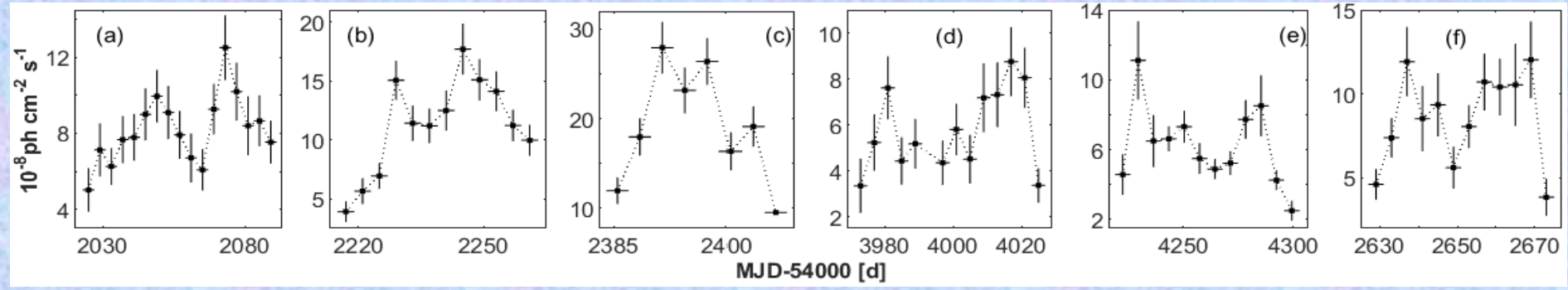

- 2012 June–September: 12 out of 25 LAT-band intra-day variability (IDV) shown by Mrk 421 since the start of the Fermi operations

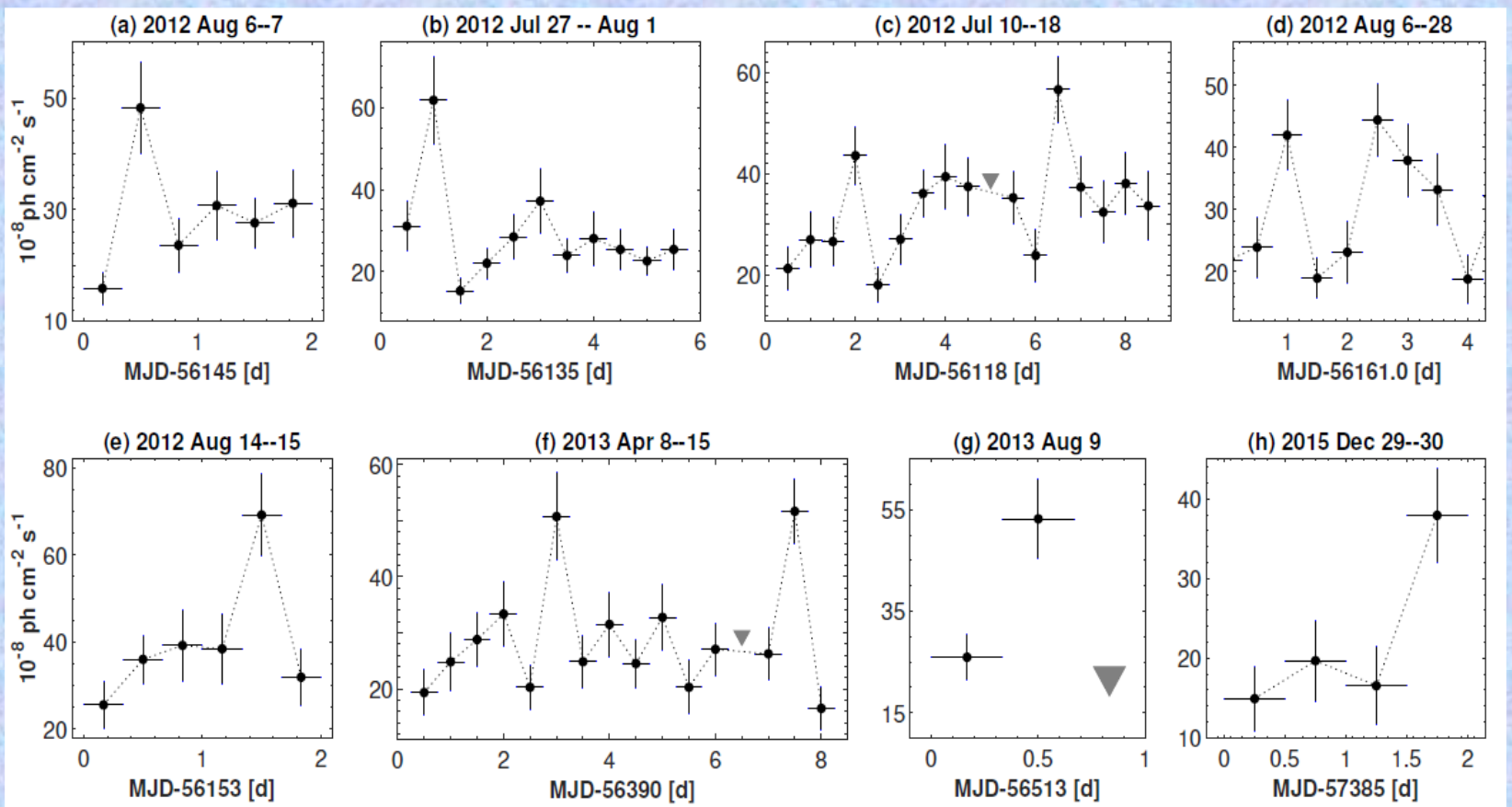

Figure 7. Selected 0.3–300 GeV IDVs. The downward gray triangles correspond to the upper limits to the LAT-band flux when $TS<9$ and/or $N_{\rm pred}<8$.

- 11 instances of the LAT-band flux doubling/halving with timescales τ_{dh}=0.43–9.65 days and fractional amplitude F_{var}=33.3(6.7)—84.7(16.3) per cent

- ✓ **LAT-band outburst in 2013 March–April**
  - Exceptionally strong 0.3–10 keV flare occurred (XRT campaign)
  - Similar behaviour recorded with Cherenkov-type telescopes and UVOT
  - Highest VHE level from the 100–500 GeV LAT data
    - ✓ Two 1-hr robust detections of the source with $F_{0.3\text{-}300\,GeV} \approx 10^{-6}$ph/cm^2/s
    - ✓ 6 instances of the 0.3-300 GeV IDVs
    - ✓ 16 instances of the LAT-band flux doubling/halving with timescales $\tau_{d,h}$=0.6–7.4 days and fractional amplitude F_{var}=32.6(5.4)–74.0(10.6) per cent
    - ✓ Moderate activity in hard X-rays (BAT&MAXI), and stronger MAXI-band activity recorded ~1 month later
    - ✓ Another strong UV-flare centered on MJD56287; no corresponding LAT-band, X-ray and optical "counterparts"
    - ✓ Strongest optical V-band flare occurring with the 0.3–300 GeV long-term declining trend.

- ✓ **Very Strong LAT-band flaring activity in 2017 December – 2018 March:**
  - ✓ Elevated baseline levels during ~4 months in the LAT, VHE, XRT, MAXI, BAT & UVOT bands
  - ✓ Mean VHE 100–500 GeV flux equal to that recorded in 2013 April (within the error ranges), with the hardest spectrum among the 13 periods of different level of LAT-band activity
  - ✓ Very strong VHE outburst by a factor of ~10 at the onset of the highest-peak short-term LAT-band flare in 2018 January, showing a peak brightness (comparable to that in 2013 April!) about one month earlier
  - ✓ Another very strong VHE flare by a factor of 8 about 3 weeks earlier - only a low amplitude HE flare in the LAT-band
    - ❖ 0.3–10 keV flux exceeding the threshold of 150 cts/s (the second highest level after the exceptionally strong X-ray flare in 2013 April)
  - However, strong simultaneous γ-ray flares in the both LAT and TeV bands in 2018 March
    - ❖ No comparable simultaneous XRT-band activity
  - UV flare in 2018 May – declined X-ray and VHE states

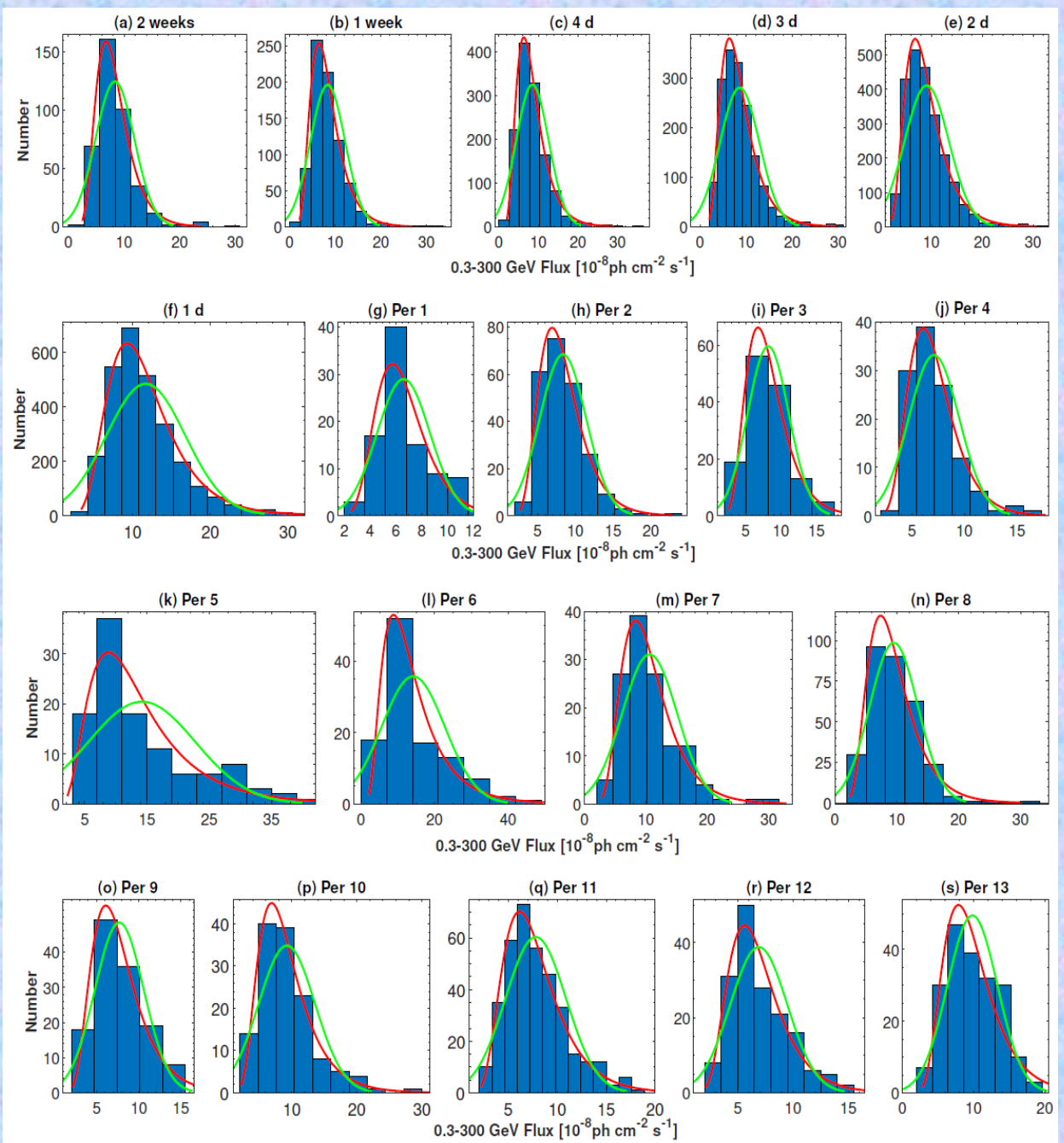

Figure 12. Distribution of the LAT-band flux values from the different time integrations (panels (a)–(f)) during 2008–2023 and that from the 2-d binned data for different periods (panels (g)–(s)). The red and green curves show the lognormal and Gaussian fits to the histograms, respectively.

- **Lognormal flux variability**

  (Rieger 2019):

  - Imprint of the accretion disk (AD) instabilities on the jet: independent density fluctuations in the AD, occurring on the local viscous timescales and characterized by a negligible damping, propagate inward and couple together ➔ Production of multiplicative behavior in the innermost disk part ➔ Generated perturbation efficiently transmitted to the jet (e.g., by means of the particle injection rate), if the timescales for particle acceleration and radiative losses within the jet are correspondingly small
  - Cascade-related emission processes (e.g., proton-induced synchrotron cascades)

✓ Distribution of the 0.3-300 GeV fluxes of Mrk 421: significantly better fit with the lognormal function compared to the Gaussian

- **Spectral properties:**
  - Few 0.3—300 GeV spectra showing a spectral curvature (~10% to 15% with different time integrations)
  - Extreme ranges of the power-law photon-index Γ in different periods

	Γ												
	Per 1	Per 2	Per 3	Per 4	Per 5	Per 6	Per 7	Per 8	Per 9	Per 10	Per 11	Per 12	Per 13
Max.	2.52(0.26)	2.76(0.27)	2.70(0.26)	2.56(0.28)	2.31(0.19)	2.38(0.22)	2.48(0.25)	2.71(0.25)	2.71(0.26)	2.64(0.29)	2.90(0.30)	2.56(0.27)	2.34(0.23)
Min.	1.24(0.12)	1.32(0.13)	1.28(0.13)	1.25(0.14)	1.51(0.07)	1.41(0.07)	1.30(0.11)	1.24(0.11)	1.27(0.13)	1.36(0.13)	1.24(0.13)	1.30(0.14)	1.29(0.13)
Mean	1.78(0.01)	1.81(0.01)	1.85(0.01)	1.81(0.01)	1.82(0.01)	1.75(0.01)	1.82(0.01)	1.76(0.01)	1.90(0.01)	1.84(0.01)	1.83(0.01)	1.87(0.01)	1.83(0.01)
Peak	1.80(0.01)	1.77(0.01)	1.87(0.01)	1.80(0.01)	1.76(0.01)	1.74(0.01)	1.77(0.01)	1.72(0.01)	1.83(0.01)	1.73(0.01)	1.78(0.01)	1.82(0.01)	1.73(0.01)

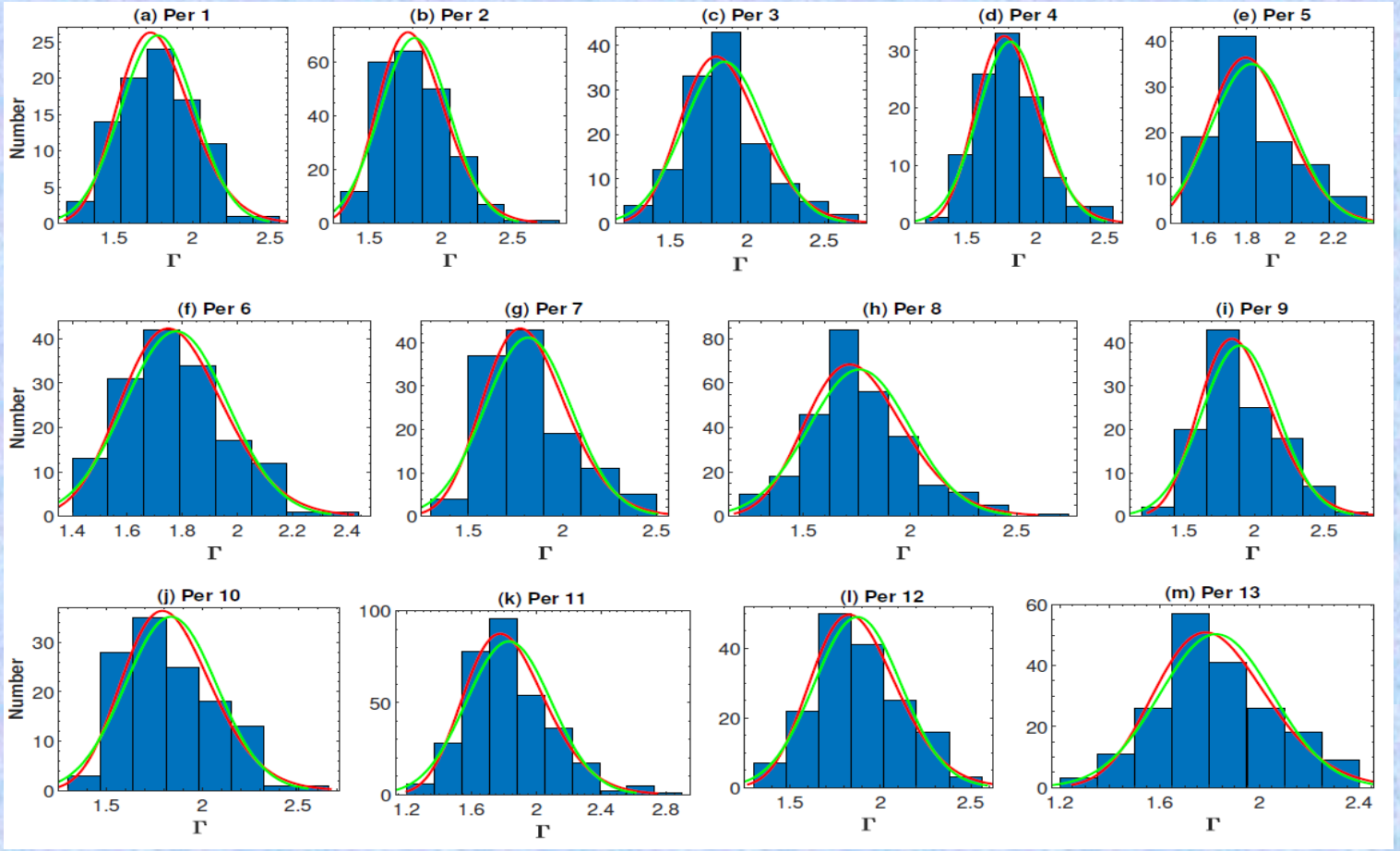

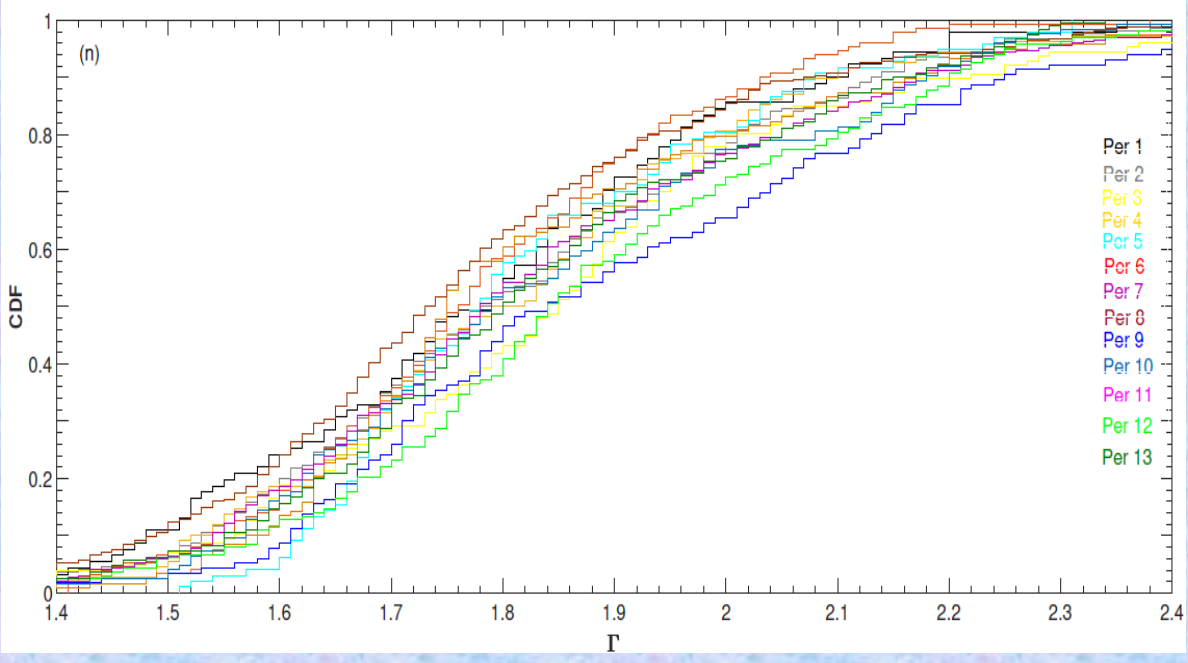

	KS	D_{KS}		KS	D_{KS}		KS	D_{KS}		KS	D_{KS}
Periods			Periods			Periods			Periods		
Per 1 vs Per 2	0	-	Per 2 vs Per 10	1	0.10	Per 4 vs Per 10	1	0.11	Per 7 vs Per 8	1	0.12
Per 1 vs Per 3	1	0.17	Per 2 vs Per 11	0	-	Per 4 vs Per 11	0	-	Per 7 vs Per 9	1	0.21
Per 1 vs Per 4	0	-	Per 2 vs Per 12	2	0.15	Per 4 vs Per 12	1	0.15	Per 7 vs Per 10	1	0.12
Per 1 vs Per 5	1	0.20	Per 2 vs Per 13	1	0.09	Per 4 vs Per 13	1	0.10	Per 7 vs Per 11	1	0.11
Per 1 vs Per 6	1	0.10	Per 3 vs Per 4	1	0.11	Per 5 vs Per 6	1	0.12	Per 7 vs Per 12	1	0.23
Per 1 vs Per 7	1	0.12	Per 3 vs Per 5	1	0.17	Per 5 vs Per 7	0	-	Per 7 vs Per 13	1	0.13
Per 1 vs Per 8	1	0.11	Per 3 vs Per 6	1	0.18	Per 5 vs Per 8	1	0.18	Per 8 vs Per 9	1	0.25
Per 1 vs Per 9	1	0.21	Per 3 vs Per 7	1	0.20	Per 5 vs Per 9	1	0.17	Per 8 vs Per 10	1	0.16
Per 1 vs Per 10	1	0.20	Per 3 vs Per 8	1	0.21	Per 5 vs Per 10	1	0.12	Per 8 vs Per 11	1	0.14
Per 1 vs Per 11	1	0.10	Per 3 vs Per 9	1	0.15	Per 5 vs Per 11	1	0.14	Per 8 vs Per 12	1	0.26
Per 1 vs Per 12	1	0.19	Per 3 vs Per 10	1	0.11	Per 5 vs Per 12	1	0.18	Per 8 vs Per 13	1	0.14
Per 1 vs Per 13	1	0.11	Per 3 vs Per 11	1	0.12	Per 5 vs Per 13	1	0.11	Per 9 vs Per 10	1	0.13
Per 2 vs Per 3	1	0.11	Per 3 vs Per 12	0	-	Per 6 vs Per 7	1	0.09	Per 9 vs Per 11	1	0.12
Per 2 vs Per 4	0	-	Per 3 vs Per 13	1	0.10	Per 6 vs Per 8	0	-	Per 9 vs Per 13	1	0.13
Per 2 vs Per 5	1	0.15	Per 4 vs Per 5	1	0.14	Per 6 vs Per 9	0	0.24	Per 10 vs Per 11	1	0.10
Per 2 vs Per 6	1	0.11	Per 4 vs Per 6	1	0.12	Per 6 vs Per 10	1	0.14	Per 10 vs Per 12	1	0.14
Per 2 vs Per 7	1	0.10	Per 4 vs Per 7	1	0.11	Per 6 vs Per 11	1	0.11	Per 11 vs Per 12	1	0.17
Per 2 vs Per 8	1	0.13	Per 4 vs Per 8	1	0.15	Per 6 vs Per 12	1	0.23	Per 11 vs Per 13	1	0.09
Per 2 vs Per 9	1	0.14	Per 4 vs Per 9	1	0.16	Per 6 vs Per 13	1	0.11	Per 12 vs Per 13	1	0.11

- Extremely hard 0.3—300 GeV spectra: up to 300 instances with Γ~1.5 or lower on timescales from intraday to 25 days: possible contribution of MeV—GeV photons having a hadronic origin?

  - Spectral hardening beyond 10 GeV – most naturally expected by significant contribution of photons from hadronic cascades (Shukla+2015)

	0.3–1 GeV			1–10 GeV			10–300 GeV		
MJDs /Date(s) (1)	N_{pred} (2)	TS (3)	Γ (4)	N_{pred} (5)	TS (6)	Γ (7)	N_{pred} (8)	TS (9)	Γ (10)
2008 Aug 5—Sep 1	108	193	1.57(0.15)	86	577	1.66(0.09)	14	198	1.37(0.12)
2008 Sep 30—Oct 27	81	133	1.91(0.23)	62	319	2.11(0.19)	12	143	1.50(0.12)
2009 Apr 14—May 11	85	161	1.89(0.20)	63	352	1.94(0.16)	16	240	1.61(0.10)
22009 Jun 9—Jul 7	114	233	2.16(0.18)	82	558	1.99(0.15)	13	152	1.72(0.12)
2009 Aug 4—31	100	240	1.53(0.14)	48	303	1.85(0.17)	11	126	1.54(0.12)
2010 May 11—Jun 7	100	196	2.14(0.18)	69	463	1.62(0.13)	13	197	1.42(0.11)
2013 Sep 24—Oct 21	114	235	1.72(0.18)	79	544	1.64(0.12)	16	193	1.37(0.12)
2014 Jan 14-Feb 10	146	285	1.83(0.16)	102	589	2.05(0.14)	15	194	1.69(0.11)
2014 Nov 18—Dec15	122	348	1.73(0.14)	92	713	1.68(0.09)	28	388	1.57(0.08)
2016 Sep 20—Oct 17	42	63	1.95(0.26)	13	35	2.72(0.38)	8	73	1.65(0.16)
2018 Jun 26—Jul 23	46	74	2.79(0.36)	25	131	1.90(0.22)	9	121	1.47(0.13)
2018 Oct 16—Nov 12	88	165	1.77(0.20)	70	439	1.87(0.17)	10	140	1.34(0.14)
2018 Dec 11—2019 Jan 07	111	194	2.18(0.19)	56	256	2.17(0.20)	17	242	1.81(0.11)
2019 Apr 2—29	102	165	2.92(0.37)	94	606	1.71(0.11)	16	264	0.97(0.20)
2019 Apr 30—May 27	62	100	1.91(0.25)	40	178	2.06(0.22)	15	253	0.93(0.20)
2019 May 28—Jun 24	116	220	1.74(0.17)	54	311	1.69(0.16)	10	124	1.31(0.14)
2019 Aug 20—Sep 16	39	73	2.62(0.36)	59	353	1.94(0.16)	8	98	1.18(0.18)
2019 Nov 12—Dec 8	142	327	1.30(0.20)	91	553	1.91(0.18)	16	202	1.29(0.12)
2020 Aug 18—Sep 14	60	124	1.83(0.24)	33	220	1.70(0.18)	8	107	1.41(0.14)
2021 Sep 14—Oct 11	92	185	1.51(0.17)	42	215	1.98(0.18)	12	130	1.50(0.12)
2022 Nov 8—Dec 5	163	332	1.94(0.15)	130	839	1.87(0.11)	24	304	1.47(0.10)
2022 Dec 6—2023 Jan 2	152	372	1.83(0.14)	93	674	1.81(0.13)	22	305	1.44(0.10)
2023 Jan 31—Feb 27	97	237	1.60(0.15)	81	541	1.82(0.15)	10	155	1.55(0.11)

- Basic hadronic scenarios for blazars:
  - Synchrotron-proton blazar (SPB) model (+ modified version): significant portion of the jet kinetic/magnetic power used to accelerate protons (& electrons) in a strongly magnetized environment to the pγ-production threshold ➔ Various synchrotron-emitting pair cascades may develop (Mannheim 1993; Cerruti et al. 2020)
    - ❖ pγ-interaction ➔ Neutral or charged pions ➔ Electrons, positrons, muon and electron neutrinos ➔ Electrons emit γ-photons (directly emitted by decay of π^0) having very high energies ➔ Third SED component after the "mutual" higher-energy "hump" to be formed (Cerruti+2015, 2020) – beyond the LAT range!
    - ❖ Proton-synchrotron emission (contributing to the lower-energy part of the γ-ray SED component; "p-synchrotron cascade") – possible contribution to the LAT range!
  - Bethe-Heitler pair production: $p + \gamma \rightarrow e^{\pm}$ ➔ Another SED "hump" to be produced, but at the lower energy compared to the "mutual one: 40 keV–40 MeV (Sol & Zech 2022) -- beyond the LAT range!

- **Relativistic magnetic reconnection** - **also producing extremely hard power-law spectra** (Sironi & Spitkovsky 2014)

- Strong currents or current sheets with non-zero electric field induced ➔ Growing instabilities and turbulences induced by the currents ➔ Development of an anomalous resistivity ➔ Magnetic field destroyed and topology altered ➔ Magnetic reconnection (Uzdensky 2006,2011)

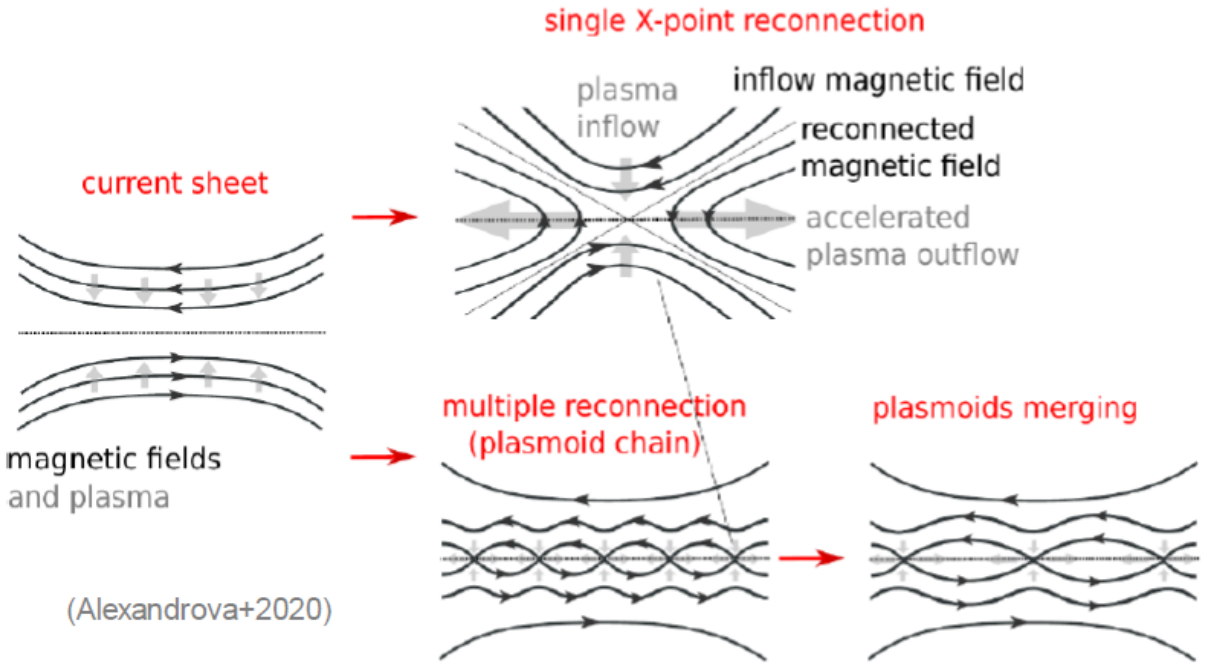

- In AGN jets, magnetic field lines can reverse on small scales due to (Zhang+2023)
  - ✓ nonlinear stages of MHD instabilities
  - ✓ jet can carry current sheets from its base
  - ✓ In both cases, field reversals on small scales are prone to magnetic reconnection
- Most reconnecting current sheets do not exhibit perfectly antialigned magnetic fields and a so-called guide present

- Astrophysical jets: reconnection in the ``**relativistic**'' regime -- magnetic energy per particle can exceed the rest mass energy (Sironi & Spitkovsky 2014)

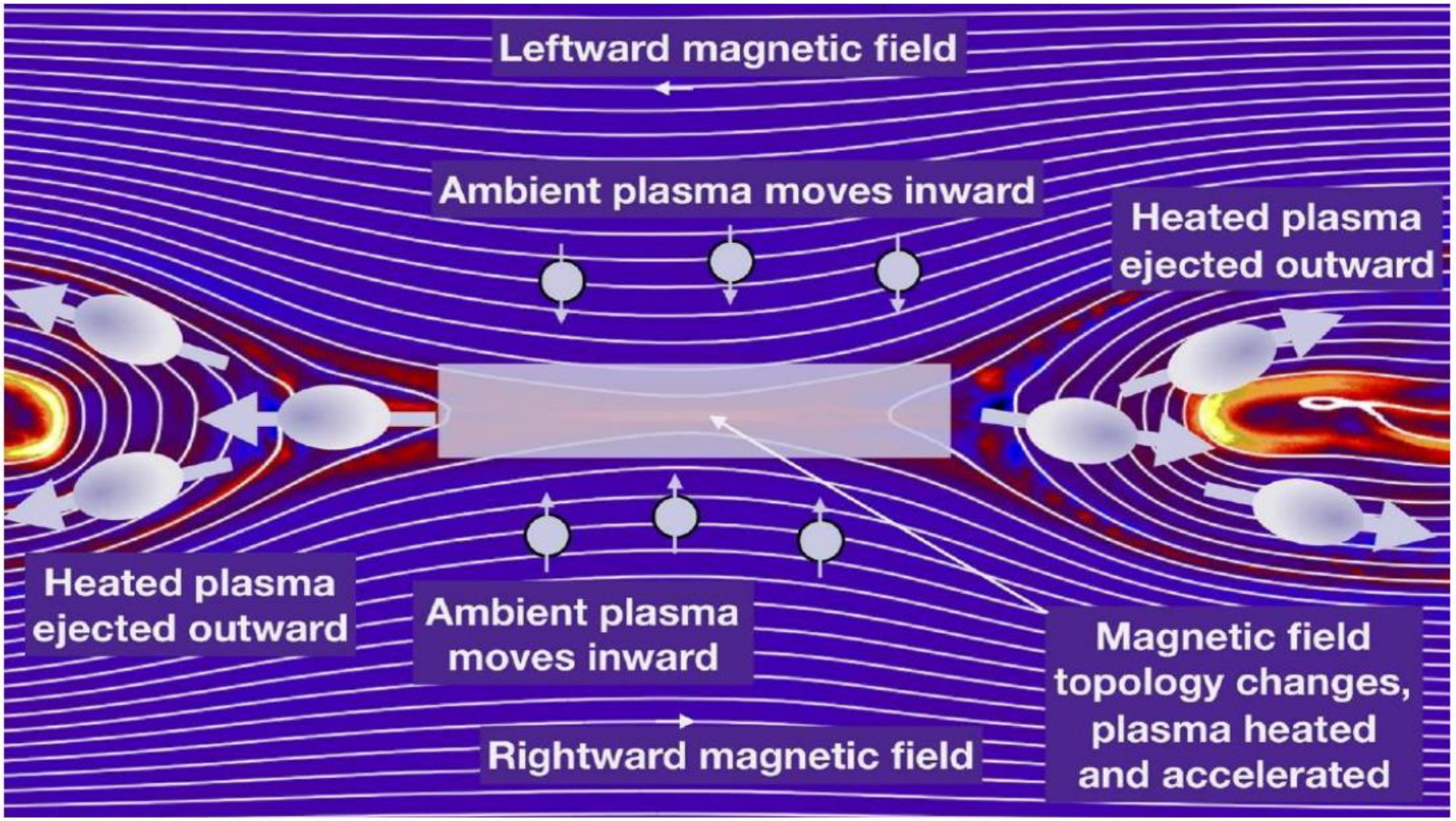

(Hesse & Cassak 2019)

- Downstream electron spectrum: two components
  - ✓ Thermal -- Maxwellian-like distribution
  - ✓ High-energy nonthermal -- PL with a high-energy cutoff $f(\gamma) \propto \gamma^{-p} e^{-\frac{\gamma}{\gamma_c}}$
- *p*-index:
  - ✓ Related to the photon index (in the νFν representation)
  - ✓ $$\Gamma = (p+1)/2$$
  - ✓ Increases with domain l_x & guide-field strength $b_g = B_g/B_0$ (B_0, reconnecting magnetic field)
  - ✓ hardens with the upstream magnetzation $\sigma_h = B_0/4\pi h$ (≡ enthalpy density of the reconnecting magnetic field divided by the relativistic enthalpy density *h* of the upstream plasma):
    - ➢ For σ_h= 50, $p \sim 1.5$ to $p \sim 3.0$ depending on b_g (French & Uzdensky 2023)
    - ➢ Frequently harder than p=4 (in contrast to 4<p<1 for σ_h= 1!)
    - ➢ **Typically hard PL** ($p \gtrsim -2$) **established when** $\sigma_{up} \gtrsim 10$ (Sironi & Spitkovsky 2014)

- ✓ **Plausible importance of the relativistic magnetic reconnection in the jet of Mrk 421: a number of the fast logparabolic ➔hard powerlaw➔logparabolic transitions from Swift-XRT spectra are detected** (Kapanadze+2024)
- ✓ **LAT-band spectra with Γ≲1.5 correspond to p≳-2 ➔ Upstream magnetization $\sigma_{up} \gtrsim 10$**

- ✓ **Upscatter in the Klein-Nishina regime**
  - **LAT-band spectral softening beyond 1 GeV or 10 GeV: IC upscatter of radio-to-optical photons in Thomson limit to lower energies vs Klein-Nishina (KN) upscatter of UV-to-Xray emission to higher GeV energies ➔ Significantly lower γ-ray outcome ("KN-suppression") ➔ Higher spectral slope**

- **Broadband SED modeling**
  - **Spectral points: LAT (Fermipy), FACT, XRT, NuSTAR, UVOT, optical & radio**
  - **Models: SSC (one/two zone), hadronic**
  - **Codes: JetSet, SOPRANO, AM^3, LeHaMoc, ….**

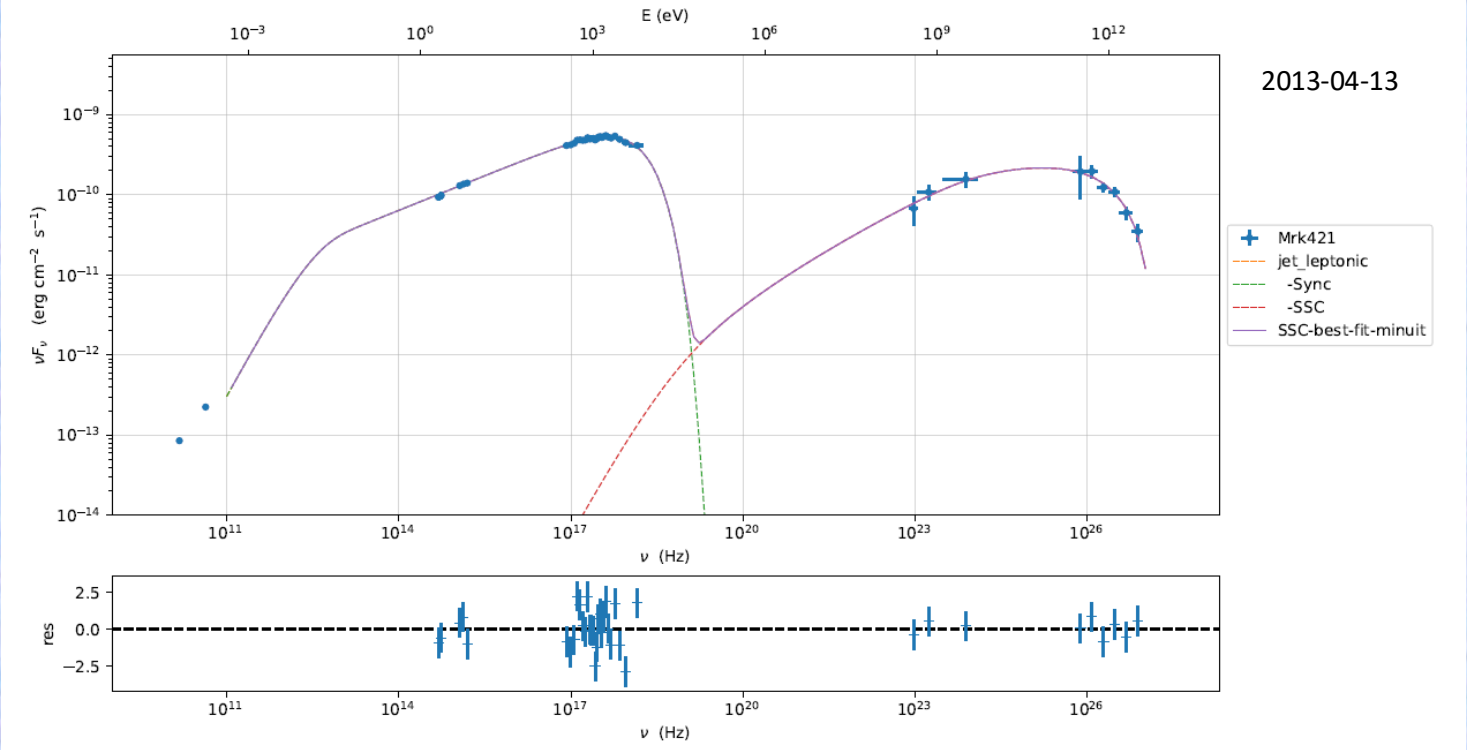

Date/MJDs	$\gamma_{\rm min}$ (10^2)	$\gamma_{\rm br}$ (10^4)	$\gamma_{\rm max}$ (10^5)	$N_{\rm e}$ ($\rm cm^{-3}$)	R ($10^{16}\rm cm$)	B (G)	δ	s	r	$\nu_{\rm p}^{\rm sync}$ ($10^{17}\rm Hz$)	$\nu_{\rm p}^{\rm IC}$ ($10^{25}\rm Hz$)	$A_{\rm C}$
(1)	(2)	(3)	(4)	(5)	(6)	(7)	(8)	(9)	(10)	(11)	(12)	(13)
2013 Mar 31/56382	5.75	6.65	5.91	1.35	7.83	0.12	8.0	2.47	0.18	4.03	1.45	0.28
2013 Apr 1/56383	9.21	9.85	11.0	1.16	3.07	0.14	14.8	2.31	0.74	3.47	0.39	0.34
2013 Apr 5–6/(5638)7–8	9.56	9.67	7.21	1.20	4.35	0.12	8.5	2.19	1.53	1.11	0.85	0.71
2013 Apr 13/56395	14.2	20.6	89.2	7.20	8.35	0.15	26.0	2.37	1.20	5.03	2.01	0.13
2013 Apr 14/56396	5.63	6.83	54.3	2.61	1.44	0.06	35.3	2.20	0.79	3.17	5.01	0.33
2013 Apr 15/56397	4.09	2.37	23.2	8.84	1.42	0.04	10.2	2.10	0.61	2.75	0.86	0.50
2014 Jan 1/56658	3.56	6.39	20.6	9.06	1.05	0.12	20.6	2.23	1.22	1.22	2.10	0.71

……

Conclusions

- Mrk 421 – bright source in the LAT band ➔ Injection and radiative evolution of freshly accelerated particles can be tracked
  - Detectable even on intraday timescales down to 0.6-1 hr during the strongest LAT-band flares in 2012 March - 2013 October and 2017 June – 2018 July (Enhanced matter collimation rate through the jet pointed to the observer?)
  - 13 periods according to the strength of the 0.3-300 GeV flaring activity (highest, strong, medium and low); different MWL timing along with LAT-band flares
    - ❖ Frequent coincidence of X-ray (XRT 0.3-10 keV, MAXI 2-20 keV, BAT 15-150 keV) and UV (UVOT UVW1, UVM2 and UVW2 bands) flares with the 0.3—300 GeV "counterparts" (with different delays: zero to several day delays) ➔ One-zone synchrotron self-Compton (SSC) scenario
    - ❖ Up to 18 flux doubling/halving instances with $\tau_{d,h}$=0.21–17.5 days ➔ Upper size of the emission zone $R_{em} \lesssim 5.3 \times 10^{15}\,\mathrm{cm} - 4.4 \times 10^{17}\,\mathrm{cm}$
    - ❖ Weaker LAT-band-to-optical correlation & radio-variability mostly uncorrelated ➔ Multi-zone SSC ?
  - Short-term LAT-band flares
    - ✓ Symmetric shape ➔ Observed variability driven by the crossing timescale of the underlying disturbance
    - ✓ Negative asymmetry: gradual acceleration of the particles responsible for the IC upscatter of low-energy photons to the MeV-GeV range
    - ✓ Positive asymmetry ➔ Nonuniformity of the Doppler factor across the jet
    - ✓ Two-peak flare: propagation of forward and reverse shocks ➔ Colliding "shells" of high-energy plasma, injected into the jet with different speeds
  - Lognormal variability – imprint of the AD instabilities onto the Mrk 421 jet
  - Occurrence of extremely hard 0.3–300 GeV spectra
    - ✓ Significant contribution of the gamma-ray photon from hadronic cascades
    - ✓ Relativistic magnetic reconnection within upstream magnetization $\sigma_{up} \gtrsim 10$
  - **Signatures of Klein-Nishina (KN) upscatter of UV-to-Xray emission to GeV energies**

Thanks! მადლობა!

Acknowledgements: B.K. thanks (1) Shota Rustaveli National Science Foundation of Georgia and E. Kharadze National Astrophysical Observatory (Abastumani, Georgia) for the fundamental research grant FR−21−307, providing a financial support to participate in the symposium; (2) organizers for the invitation and hospitality